Bacterial Adhesion and Biofilm Formation: Hydrodynamics Effects

Luciana C. Gomes, Rita Teixeira-Santos, Maria J. Romeu, and Filipe J. Mergulhão

Abbreviations

3-D	Three-dimensional
AUM	Artificial urine medium
CFD	Computational fluid dynamics
CLSM	Confocal laser scanning microscopy
FC	Flow chamber
MRD	Modified Robbins device
PDMS	Polydimethylsiloxane
PPFC	Parallel-plate flow chamber
RD	Robbins device
UTD	Urinary tract device
UTI	Urinary tract infection

L. C. Gomes · R. Teixeira-Santos · M. J. Romeu
LEPABE-Laboratory for Process Engineering, Environment, Biotechnology and Energy, Faculty of Engineering, University of Porto, Porto, Portugal
e-mail: luciana.gomes@fe.up.pt; ritadtsantos@fe.up.pt; mariaromeu@fe.up.pt

F. J. Mergulhão (✉)
LEPABE-Laboratory for Process Engineering, Environment, Biotechnology and Energy, Faculty of Engineering, University of Porto, Porto, Portugal

ALiCE-Associate Laboratory in Chemical Engineering, Faculty of Engineering, University of Porto, Porto, Portugal
e-mail: filipem@fe.up.pt

F. Soria et al. (eds.), *Urinary Stents*,
https://doi.org/10.1007/978-3-031-04484-7_19

1 Introduction

The complications associated with indwelling ureteral stents, namely bacterial adhesion and biofilm formation, have been the main driving force for the development of new materials or coatings with antimicrobial and anti-adhesive properties. The first approach for testing and optimizing new biomedical surfaces usually consists of evaluating their *in vitro* efficacy under controlled experimental conditions that reflect the human physiological environment [1]. Consequently, several parameters, including the pathogenic species and their concentration, culture medium, temperature, and hydrodynamic conditions, must be considered when setting an *in vitro* experiment, hence increasing its predictive value and avoiding, during initial screening, expensive *in vivo* assays and animal sacrifice [1] without prior evidence of surface effectiveness. Among these parameters, hydrodynamic conditions have a prominent role in the experimental setup as assays performed in static conditions do not mimic the fluid flow that occurs at specific locations of the human body (e.g. urinary tract). Furthermore, it is well known that hydrodynamic conditions affect not only bacterial adhesion to biomedical surfaces [2], but also biofilm growth and architecture [3, 4]. In fact, flow determines the transport rate of planktonic cells to the surface and their subsequent interaction [5], as well as the transport of oxygen and nutrients to the biofilm [6]. Besides, flow influences both bacterial attachment and detachment rates [7].

The effectiveness of biomedical surfaces may also be highly affected by the hydrodynamic conditions [1]. Surfaces releasing antimicrobial substances when exposed to flow may exhibit shorter lifetimes than at static conditions [1]. Likewise, depending on the fluid flow surrounding the surface, contact-killing surfaces that are adhesive for bacterial cells may be covered by bacterial debris, which decreases their antimicrobial activity [1]. Lastly, non-adhesive coatings, such as polymer brush coatings, are generally sensitive to external stimuli, exhibiting higher antifouling performance at quasi-static conditions and more effective fouling release behavior under dynamic conditions [8].

Considering the importance of hydrodynamic conditions and their effects on bacterial adhesion and biofilm formation, a diversity of *in vitro* flow systems, including the Robbins device (RD) and modifications, the drip flow biofilm reactor, rotary biofilm reactors and flow chambers (FCs), have been developed and optimized to evaluate surfaces effectiveness under physiological conditions [9]. Certain flow systems enable real-time visualization of bacteria adhesion/biofilm development under controlled conditions (e.g. shear stress or shear rate, temperature), allow simultaneous testing of different materials, and can be used as high-throughput platforms [9], while others have some limitations in operating at highly controlled hydrodynamic conditions [1]. Hence, each platform presents advantages and disadvantages that must be considered before use.

In this chapter, the most commonly used platforms for the *in vitro* assessment of bacterial adhesion and biofilm formation under flow conditions—the modified Robbins device, flow chambers, and microfluidic devices—are introduced, and their

main advantages and disadvantages discussed. These three testing platforms have been particularly used to evaluate the anti-adhesive and antibiofilm performance of novel surface materials for urinary tract devices (UTDs), including catheters and stents, due to their ability to control the hydrodynamics (shear stress and flow rate) and recreate *in vivo* flow conditions.

2 Robbins Device and Modifications

The Robbins device was initially developed by Jim Robbins and Bill McCoy to study biofilm formation in industrial water systems [10]. The RD consists of a pipe with several holes where coupons are mounted on the end of the screws and become in contact with the fluid. Thus, the RD generates submerged biofilms growing in aqueous systems that can be used for the investigation of multispecies communities [10].

Several modifications were later introduced to this design, including the use of a square-channel pipe where coupons are aligned with the inner surface without disturbing flow characteristics [11]. Other designs include a half-pipe geometry that more closely resembles the circular section of a tube [4]. With the modified Robbins devices (MRDs), the flow can be momentarily stopped to allow direct access to the coupons so that time-course experiments are also possible [3].

MRDs have been operated in conditions that mimic the flow in urinary catheters [12, 13] and stents [13, 14]. Tunner et al. [14] were among the first authors to use a continuous flow model based on an MRD to assess encrustation on silicone and polyurethane, the most widely used ureteral stent biomaterials. They revealed that the type and degree of encrustation produced were similar to those found *in vivo*, recommending this flow system for comparative evaluation of surface candidates for medical devices used in the urinary tract [14]. More recently, in our research group, a MRD (referred to as flow cell system) simulating the hydrodynamic conditions found in urinary catheters (shear rate of 15/s) [15] was used to characterize the microbial physiology of *Escherichia coli* and *Delftia tsuruhatensis* individually and in a consortium, in terms of growth kinetics and substrate uptake, when exposed to artificial urine medium (AUM) flow and silicone material [12]. Additionally, we used a custom-made semi-circular flow cell identical to that shown in Fig. 1 to assess the efficacy of different nanocomposite coatings in preventing urinary tract infections (UTIs) [13]. The hydrodynamics of this flow cell was fully characterized by computational fluid dynamics (CFD) [16], and it has been shown that the shear stress field is approximately the same in the curved and flat walls so that coupons can be placed on the flat wall for convenience and still be subjected to the same shear forces acting on the curved wall [17]. Moreover, this flow cell was constructed to have enough inlet length to allow for full flow development and a large surface area on which the hydrodynamic conditions remain constant for a wide range of flow velocities [16]. These dynamic systems are particularly useful for screening purposes as they enable the simultaneous testing of several surfaces [13, 14].

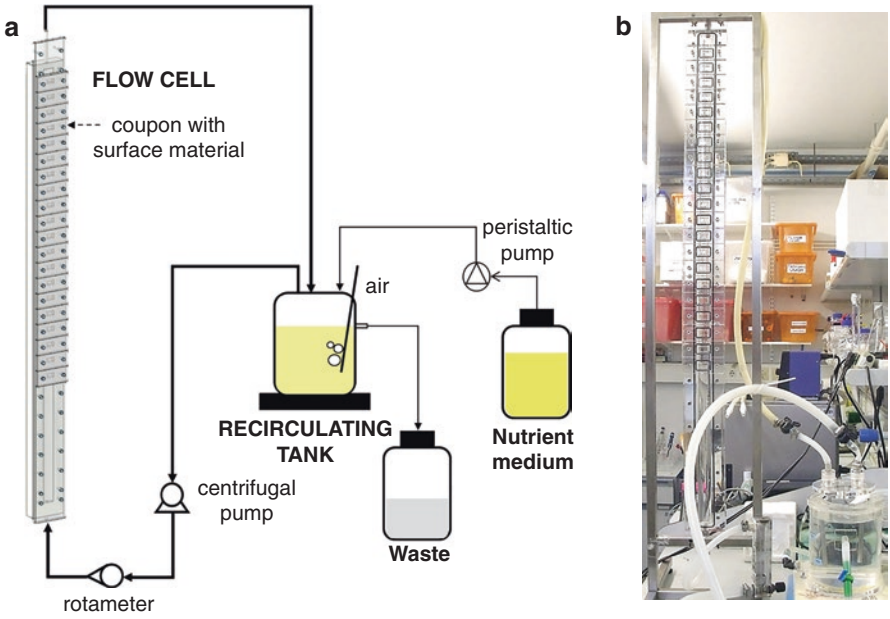

Fig. 1 (**a**) Schematic representation and (**b**) photograph of a MRD. The system is mainly composed by a recirculating tank, one vertical semi-circular flow cell (about a meter high) with removable coupons, and peristaltic and centrifugal pumps

Another advantage of MRDs is that coupons can be removed independently, for instance, at different experimental times [12].

3 Flow Chamber

Despite the many advantages of the MRDs, they are usually not suited for direct analysis of biofilm development [18], and they are not adequate to monitor cell adhesion to a surface. Nowadays, there are several models of flow chambers that can be mounted on a microscope stage and used with video capture systems, enabling real-time observation of microbial adhesion, particularly when used with transparent surfaces [18]. Different custom-made FCs have been used to evaluate the anti-adhesive and antibiofilm properties of novel surfaces for UTDs, namely catheters and stents, in flow conditions that simulate those typically found in these medical devices [2, 15, 19, 20]. Table 1 summarizes several studies found in the literature where flow chamber assays were performed under fully characterized hydrodynamic conditions similar to those of urinary catheters and stents. Most of these studies aimed to monitor the initial adhesion of bacteria associated with UTIs (*E. coli*, *Enterococcus faecalis, Staphylococcus aureus* and *Pseudomonas aeruginosa*) to polymeric surfaces as polydimethylsiloxane (PDMS) [2, 9] and PDMS modified

Table 1 Flow chamber studies to evaluate the initial adhesion and biofilm formation under hydrodynamic conditions identical to those found in UTDs

Study aim	Surface material	Microorganisms	Culture conditions (medium, cell concentration, flow rate and/or Re, and time)	Shear stress and/or shear rate values	Major conclusions	Refs.
Initial adhesion	Smooth PDMS, smooth PDMS with peptide coating, micropatterned PDMS and micropatterned PDMS with peptide coating	*E. coli*	AUM 7.6×10^7 cells/mL $Q = 2$ and 4 mL/s 30-min assay	0.010 and 0.024 Pa	The highest *E. coli* adhesion was obtained on the smooth PDMS, whereas the micropatterned PDMS coated with peptide totally inhibited adhesion. The peptide addition to the smooth PDMS reduced the adhesion by 43–58%, while the micropatterned PDMS reduced the adhesion by 99%.	[21]
	PDMS and CNT/PDMS composites	*E. coli*	Citrate buffer 7.6×10^7 cells/mL $Q = 2$ mL/s 30-min assay	0.010 Pa 15/s	Introduction of the CNTs in the PDMS matrix yielded less bacterial adhesion than the PDMS alone. Less adhesion was obtained on the composites with pristine rather than functionalized CNTs. Incorporation of higher amounts of CNTs in polymer composites can affect bacterial adhesion by more than 40%. Composites enabling a 60% reduction in cell adhesion were obtained by CNT treatment by ball-milling.	[22, 23]
	Glass, poly(HPMA) and poly(MeOEGMA) brushes	*E. coli*	Citrate buffer 7.6×10^7 cells/mL $Q = 2$ and 4 mL/s 30-min assay	0.010 and 0.024 Pa	The poly(MeOEGMA) and poly(HPMA) surfaces reduced the initial adhesion up to 90% when compared to glass.	[58]
	Glass, peptide-coated glass and PLLA	*E. coli*	Citrate buffer and enriched medium 7.6×10^7 cells/mL $Q = 2$ and 4 mL/s 30-min assay	15 and 30/s	Adhesion reductions of 40–50% were attained at a shear rate of 15/s on the peptide-coated surfaces compared with bare glass. The performance of the peptide-based antifouling coating was superior to PLLA.	[26]
	Glass, PDMS and PLLA	*E. coli*	Citrate buffer 7.6×10^7 cells/mL $Q = 2$ and 4 mL/s 30-min assay	0.01 and 0.022 ± 0.002 Pa (equivalent to 32/s)	Similar adhesion rates were obtained on glass and PDMS. The highest adhesion rates were obtained on glass and PDMS and the lowest on PLLA.	[2, 9]

(continued)

Table 1 (continued)

Study aim	Surface material	Microorganisms	Culture conditions (medium, cell concentration, flow rate and/or Re, and time)	Shear stress and/or shear rate values	Major conclusions	Refs.
	Silicone wafers, silicone rubber and PAAm brushes	*S. aureus* *Strep. salivarius* *C. albicans*	PBS or saliva 3×10^8 bacteria/mL and 3×10^6 yeast/mL 4-h assay	10/s	A high reduction (52–92%) in microbial adhesion to the surface-grafted PAAm brush was observed as compared with untreated silicon surfaces. PAAm brush coatings on silicone rubber inhibited microbial adhesion as well as PAAm brushes grafted from silicon wafers.	[59, 60]
	Glass and PEO-coated glass slide	*S. epidermidis* *S. aureus* *Strep. salivarius* *E. coli* *Ps. aeruginosa* *C. albicans* *C. tropicalis*	PBS 3×10^8 bacteria/mL and 3×10^6 yeast/mL $Q = 0.025$ mL/s 4-h assay	10/s	The PEO brush yielded more than 98% reduction in bacterial adhesion, although for the more hydrophobic *Ps. aeruginosa* a smaller reduction was observed. For yeast species, adhesion suppression was less effective than for the bacteria, and here the more hydrophobic *C. tropicalis* showed less reduction than the more hydrophilic *C. albicans*.	[61]
	Silicone rubber	UTI isolates: *E. coli* *Ent. faecalis* *S. epidermidis* *Ps. aeruginosa* *C. albicans*	Human urine 3×10^8 bacteria/mL and 3×10^6 yeast/mL $Q = 0.034$ mL/s 4-h assay	15/s	Cranberry and ascorbic acid supplementation can provide a degree of protection against adhesion and colonization of biomaterials by some uropathogens.	[20]
	Glass or silicone rubber coated with different concentrations of a biosurfactant	*Ent. faecalis*	PBS or pooled human urine 3×10^8 cells/mL $Q = 0.034$ mL/s $Re = 1$ 4-h assay	15/s	Biosurfactant layers greatly inhibited the initial deposition rates (> 30%) and adhesion numbers (≈ 70–100%) in a dose-related way. This inhibition was stronger when buffer was used. For urine experiments, biosurfactant coatings on silicone caused higher adhesion reductions.	[15]
	Glass and FEP	*Ent. faecalis*	PBS or pooled human urine 3×10^8 cells/mL 4.5-h assay	15/s	*Ent. faecalis* was displaced by lactobacilli (31%) and streptococci (74%) from FEP in buffer and that displacement by lactobacilli was even more effective on glass in urine (54%). The passage of an air–liquid interface significantly impacted adhesion, especially when the surface had been challenged with lactobacilli (up to 100%) or streptococci (up to 94%).	[62]

Biofilm formation	PDMS, glass and the poly(HPMA) brush	*E. coli*	AUM 7.6×10^7 cells/mL $Q = 2$ mL/s 24 h biofilm formation (infection period) + 8 h fresh medium exposure (post-infection period)	15/s	Initial adhesion and surface coverage decreased on poly(HPMA) brush. This antifouling behavior was maintained during infection and post-infection period, when the reduction in total cell number reached 87%. VBNC cells were completely removed from the brush. Poly(HPMA) may reduce biofilm growth and antibiotic resistance in urinary catheters.	[19]
	PDMS, glass and poly(MeOEGMA) brush	*E. coli*	AUM 7.6×10^7 cells/mL $Q = 2$ mL/s 24 h biofilm formation +8 h antibiotic treatment	15/s	The polymer brush reduced by 57% the surface area covered after 24 h, as well as the number of total adhered cells. The antibiotic treatment potentiated cell death and removal (88%). Poly(MeOEGMA) brush has the potential to prevent biofilm growth in UTDs, and in eradicating biofilms developed in these devices.	[24]
	Platinum electrodes	*P. mirabilis*	AUM 2×10^6 CFU/mL $Q = 3333$ mL/s 6 days	200/s	By applying alternating microcurrent densities, a self-regenerative surface is produced, which actively removed the conditioning film and significantly reduced bacterial adherence, growth, and survival.	[63]
	Silicone and silicone coated with ppVP	*E. coli* UTI isolates *E. coli* standard strain	Peptone-glucose nutrient medium 1×10^6 CFU/mL $Q = 4 \times 10^{-3}$ mL/s $Re = 1.19$ 20–24 h	33/s	The temperature had a considerable influence upon the adhesion and biofilm-forming capacity of some of the isolates, and the influence of surface chemistry depended on temperature.	[25]

AUM artificial urine medium, *CNT* carbon nanotube, *FEP* fluorinated ethylene propylene, *PBS* phosphate-buffered saline, *PEO* poly(ethylene oxide), *PLLA* poly-L-lactic acid, *PAAm* polyacrylamide, *poly(HPMA)* poly[*N*-(2-hydroxypropyl) methacrylamide], *poly(MeOEGMA)* poly[oligo(ethyleneglycol) methyl ether methacrylate], *PDMS* polydimethylsiloxane, *ppVP* plasma polymerized vinylpyrrolidone, *Q* flow rate, *Re* Reynolds number, *UTDs* urinary tract devices, *VBNC* viable but nonculturable, *C. Candida*, *Ent. Enterococcus*, *E. Escherichia*, *P. Proteus, Ps. Pseudomonas*, *S. Staphylococcus*, *Strep. Streptococcus*

with antimicrobial substances (peptides and carbon nanotubes) [21–23] for 30 min to 4 h. In some instances, these systems were also used to investigate bacterial biofilm growth and survival for 24 h on novel surface coatings for UTDs [19, 24, 25].

A custom-made FC system (Fig. 2) was designed by our group to analyse cell adhesion [22, 26] and biofilm formation [19, 24]. This system includes a parallel-plate flow chamber (PPFC) coupled to a jacketed tank and connected to centrifugal pumps and a valve by a silicone tubing system. The valve allows the bacterial suspension to circulate through the system at a controlled flow rate, and the recirculating water bath is connected to the tank jacket to enable temperature control. To illustrate the type of data that can be obtained with this platform, biofilm formation experiments with *E. coli* were carried out for 24 h using PDMS as the test surface [27] and AUM recirculated through the FC system at 4 mL/s to mimic the urine flow behavior in ureteral stents (shear rate of 15/s). After 24 h, the system was stopped, and the biofilm formed on the PDMS surface was stained with a fluorescent dye and analysed by confocal laser scanning microscopy (CLSM) (Fig. 3 and Table 2).

CLSM is an optical imaging technique used to obtain high-resolution images of biofilms at various depths in their naturally hydrated form and to generate three-dimensional (3-D) reconstructions of the samples [28]. It is particularly well suited for monitoring 3-D structure formation in flow chamber-grown biofilms due to its non-invasive and non-destructive character [29, 30]. Early research investigating the use of CLSM in biofilm studies was more descriptive, using qualitative metrics to evaluate biofilm architecture [31]. The development of imaging software packages, specifically for biofilm samples, has enhanced the quantitative output from CLSM images of biofilms [32]. Among these, the COMSTAT ImageJ plugin [32] used in the present work (Table 2) or the PHLIP Matlab toolbox [33, 34] represent a set of reference tools that are efficient and reliable to characterize biofilms in terms of biomass, thickness distribution, surface coverage, roughness coefficient, or porosity.

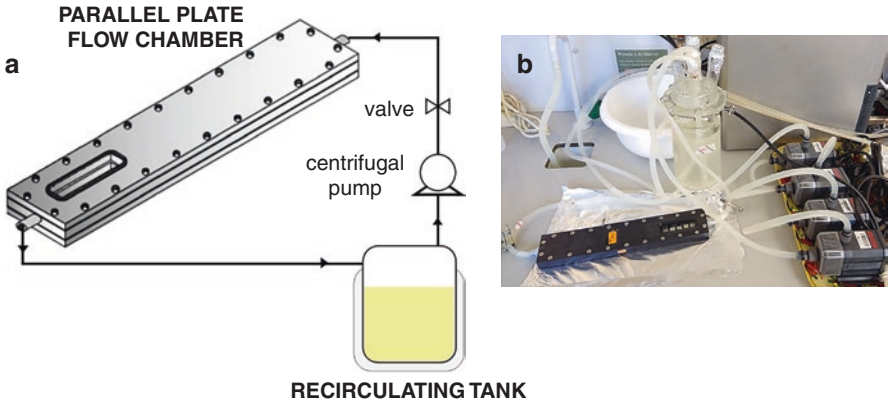

Fig. 2 (**a**) Schematic representation and (**b**) photograph of the FC system. The PPFC is coupled to a glass tank connected to four centrifugal pumps and a tubing system to conduct adhesion or biofilm formation assays

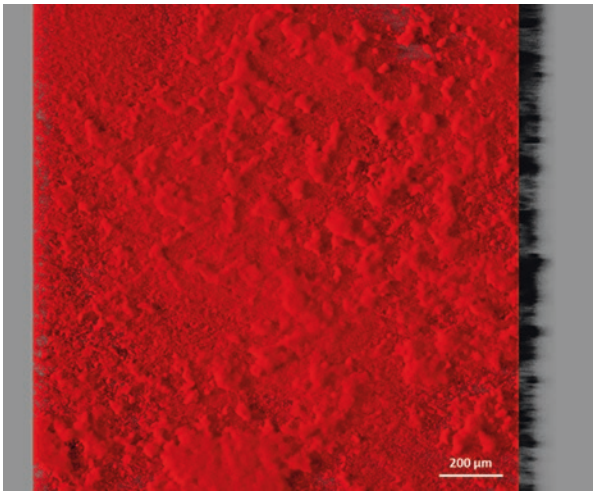

Fig. 3 3-D projection of biofilms formed on PDMS at a flow rate of 4 mL/s mimicking ureteral stents in the described PPFC system. Shown is an *E. coli* biofilm stained with SYTO 61 (633 nm laser line, LEICA HCX PL APO 10 ×/0.40 CS). This representative image was obtained using the "Easy 3D" tool of IMARIS 8.4.1 software (Bitplane, Switzerland) from a confocal *z* stack, and presents an aerial view of the biofilm structure with the shadow projection on the right

Table 2 Quantified data for *E. coli* biofilms grown on PDMS surfaces in the PPFC system. These parameters were obtained from confocal image series using the COMSTAT2 tool associated with the ImageJ software. The means (± standard deviations) for three independent experiments are presented

Biofilm parameters	
Biovolume ($\mu m^3/\mu m^2$)	29.99 (± 2.23)
Average thickness (µm)	72.99 (± 6.94)
Roughness coefficient	0.20 (± 0.02)

4 Microfluidic Devices

Microfluidic platforms have demonstrated high potential and versatility for the study of bacterial adhesion and biofilm formation under different growth conditions. These platforms allow the testing of different channel architectures and types of materials or surfaces at highly controlled flow conditions through a rapid and precise analysis [5]. For these reasons, microfluidic platforms have been used to explore the combined effect of several factors on the development of clinically relevant biofilms [35–37]. Table 3 lists several studies using microfluidic devices for the evaluation of bacterial adhesion and biofilm formation under flow conditions that represent relevant hydrodynamic regions of ureteral stents.

Although microfluidic devices can be constructed by different methodologies and from a diversity of materials, PDMS has been the material of choice for the construction of these devices, with most of the PDMS-based microfluidic devices

Table 3 Microfluidic platforms used for the study of bacterial adhesion and biofilm formation under hydrodynamic conditions identical to those found in ureteral stents

Microfluidic platform	Surface materials	Study aim	Microorganisms	Shear stress and/or shear rate values	Major conclusions	Refs.
PDMS-based microfluidic device	PDMS glass	Early-stage bacterial adhesion (25 min)	*Ps. aeruginosa*	0.05–10 Pa	The residence time increased with increasing shear stress linearly over a wide range of shear stresses (0.05–3.5 Pa).	[7]
	PA PDMS PEO PLLA PS	Development of a fabrication method to produce a microfluidic device to test cell adhesion (1800 s)	*E. coli*	0.01–1 Pa	Bacterial adhesion increased linearly over time. The evaluation performed with PDMS surfaces for shear stresses between 0.02 and 1 Pa showed that the lowered surface (inherent weakness of the fabrication method) did not influence adhesion.	[38]
	Glass	Short-term bacterial adhesion (1800 s)	*E. coli*	0.2–10 Pa	Bacterial adhesion increased in locations with a sudden increase in shear stress.	[39]
	Glass	Short-term bacterial adhesion (1 h)	*B. subtillis* *Ps. aeruginosa*	Up to 100/s	The flow produced a strong spatial heterogeneity in bacterial concentration, characterized by up to 70% cell depletion from low-shear regions due to "trapping" in high-shear regions. The maximal depletion occurred at intermediate shear rates. Surface coverage increased with increasing shear rate up to 20/s.	[40]
	PDMS	Short-term bacterial adhesion (1 h) in urinary stents	*Ps. fluorescens*	Up to 0.175 Pa	The unobstructed device showed no short-term bacterial attachment, including in regions of low WSS (< 0.04 Pa). For the obstructed devices, the cavity region, and the nearby proximal side-hole (WSS of 0.131–0.175 Pa) exhibited greater levels of bacterial attachment (18 ± 3%) compared to other regions of the model.	[5]
	PDMS	Bacterial attachment on curved surfaces (5 h)	*E. coli* *Ps. aeruginosa*	Up to 40/s	The bacterial attachment to a curved surface depends on the flow and in slower flow conditions can be up to two-fold higher.	[41]
	Glass	Initial biofilm formation (11 h)	*E. coli*	1.67, 8.33, 83.3 and 166.6/s	Bacteria were able to form communities at 8.33, 83.3, and 166.6/s. However, the multilayer growth was only visible at 166.6/s after 10 h.	[43]

	Glass	Evaluation of bacterial colonization, competition, and dispersal (15 h)	*Ps. aeruginosa* *B. subtilis* *E. coli* *P. mirabilis* *S. aureus* *Sa. typhimurium*	0.02–2 Pa	The upstream movement was a direct response to surface shear stress and conferred to *Ps. aeruginosa* selective growth advantages.	[42]
	Glass	Biofilm formation (24–48 h)	*Ps. aeruginosa*	0.002–0.014 Pa	Biofilm thickness was not affected by shear stress after 24 h, displaying on average 10 μm. At 48 h, the biofilm thickness increased significantly (36 ± 9 μm) at 0.010 Pa and slightly at 0.0035 Pa (20 ± 4 μm). Contrary, no increase was observed for higher shear stress.	[44]
	Uncoated and HBP-coated channels	Biofilm formation (16 h)	*S. aureus*	0.02–1 Pa	The flow was the major contributor to the shape of biofilm structures, whereas bacterial motility was less significant.	[45]
	Channels coated with fibronectin solution from humans	Influence of constant or intermittent flow on QS-mediated communication during biofilm formation (16 h)	*S. aureus* *Vibrio cholerae*	0.003–0.3 Pa	QS was generally repressed by the flow. However, it could be locally activated in the downstream location of long channels and within the crevices of a groove-like surface.	[48]
	Channels treated with octyl(tri-ethoxy)silane	Biofilm formation on intravascular catheters microenvironment (24 h)	*S. epidermidis*	0.065–1.14 Pa	Fluid shear alone induced the formation of polysaccharide intracellular adhesin-positive biofilms and influenced the biofilm structure.	[46]
	Electrode surfaces	The effect of hydrodynamic stress on biofilm formation (71 h)	*P. fluorescens*	0.00535–0.0535 Pa	The complete removal of significant portions of biofilm outer layers occurred after the application of extreme shear stress and the structure of the remaining biofilm was susceptible to further changes.	[47]
	PDMS	Biofilm growth and detachment (120 h)	*S. epidermidis*	0.01–0.15 Pa	*S. epidermidis* biofilm formation was affected by the local hydrodynamics conditions. Higher WSS conditions limited vertical biofilm growth, resulting in a monolayered structure, while cells growing in stagnant areas were able to divide and proliferate more freely, resulting in the formation of a large multilayered structure.	[35]

(continued)

Table 3 (continued)

Microfluidic platform	Surface materials	Study aim	Microorganisms	Shear stress and/or shear rate values	Major conclusions	Refs.
BioFlux microfluidic system	Glass	Biofilm formation (15 h)	*A. baumannii*	0.2 Pa	Bacteria attached to the glass surface at the start of the flow stayed attached and did not relocate.	[52]
	Glass	Gene expression during biofilm formation (18 h)	*S. aureus*	0.06 Pa	The *cid* and *lrg* expression was impaired during biofilm development under static conditions compared to flow conditions due to the hypoxic nature of static biofilms.	[49]
	Glass (dynamic) Polystyrene (static)	Biofilm formation (18 h)	Methicillin-resistant *S. aureus*	0.05 Pa	From tested isolates, 51% successfully formed biofilms under shear flow. However, differences in biofilm formation might also be due to the different adherent surfaces used in the static and dynamic systems.	[53]
	Glass	Gene expression during biofilm formation (18 h)	*S. aureus*	0.06 Pa	lytS and lytR deletion mutations did not have a visible effect on biofilm structure under microfluidic conditions, while LytR overactive strains induced differences in average biomass, average thickness, and roughness of biofilms formed under static conditions. The biofilm phenotypic differences may be related to the oxygen concentration in dynamic and static conditions.	[50]
	Glass and eukaryotic cells (HRT-18)	Biofilm formation (24 h)	*E. coli*	0.05–1 Pa	Biofilm formation on glass was observed for the most strains when they were grown in M9 medium at 30 °C but not in RPMI. Similar results were obtained for static conditions. HRT-18 cell monolayers enhanced *E. coli* binding and biofilm formation in RPMI medium.	[36]
	Glass	Effect of weaker biofilm-forming CNS isolates on the biofilm formation of other staphylococcal isolates (24 h)	Coagulase-negative staphylococci	0.05 Pa	CNS with weak-biofilm phenotype did not inhibit the growth of isolates with a strong-biofilm phenotype either under static or flow conditions.	[54]

CNS coagulase-negative staphylococci, *HBP* human blood plasm, *PA* polyamide, *PDMS* polydimethylsiloxane, *PEO* polyethylene oxide, *PLLA* poly-*l*-lactide acid, *PS* polystyrene, *QS* quorum sensing, *WSS* wall shear stresses, *A. Acinetobacter, B. Bacillus, E. Escherichia, P. Proteus, Ps. Pseudomonas, S. Staphylococcus, Sa. Salmonella*

being designed for a specific purpose. Several studies have investigated the initial bacterial adhesion on different materials using microfluidic platforms [5, 7, 38–41]. In general, the bacterial residence time and surface coverage increased linearly up to 3.5 Pa [7] and 20/s [40], respectively, and the adhesion rates were higher in locations with a sudden increase in shear forces [39]. For the particular case of ureteral stents, De Garcia et al. [5] demonstrated that unobstructed devices (wall shear stress ≤ 0.0875 Pa) showed no short-term bacterial adhesion, while in obstructed devices, the cavity region and nearby proximal side-hole (wall shear stress of 0.131–0.175 Pa) exhibited higher levels of bacterial attachment compared to other regions of the model. Although channel architecture and geometry affect bacterial adhesion [41], these findings indicate that flow influences both attachment and detachment rates [7].

PDMS-based microfluidic devices have also been applied to explore how bacterial colonization, competition, and dispersal occur at flow conditions. Indeed, flow can confer growth advantages to pathogens by allowing the bacteria upstream movement [42]. Similarly, the study of biofilm development is also possible using these microfluidic platforms [35, 43–48]. Several authors revealed that flow alone was able to induce the formation of polysaccharide intracellular adhesins [46] and was the major modulator of the biofilm structures [45]. Additionally, Lee et al. [35] demonstrated that the morphology of *Staphylococcus epidermidis* biofilm formation was influenced by local hydrodynamic conditions. While higher wall shear stress limited vertical biofilm growth, resulting in a monolayer structure, cells growing in stagnant areas were able to proliferate rapidly, resulting in the formation of a large multilayer structure [35]. Likewise, biofilm thickness was also affected by flow after 48 h, increasing significantly at 0.010 Pa (36 ± 9 μm) and slightly at 0.0035 Pa (20 ± 4 μm). Contrarily, no increase was detected for higher shear stresses [44]. Accordingly, Kim et al. [48] revealed that quorum sensing-mediated communication during biofilm formation was generally repressed by flow, impairing biofilm growth. The comprehensive analysis of gene expression during *S. aureus* biofilm formation was successfully conducted by Moormeier et al. [49, 50] using a different microfluidic device, the BioFlux system (Fluxion Systems, South San Francisco, CA), and compared with static conditions. The BioFlux system was presented as the most prominent commercial microfluidic platform that overcomes the limitations of static well plates and conventional laminar flow chambers. In this system, biofilm formation can be followed by light microscopy in microfluidic wells, allowing rapid screening of the effects of several compounds on the viability of biofilms under hydrodynamic conditions [51]. One of the early studies performed on this platform evaluated the effect of several antimicrobials on 8 h-developed *P. aeruginosa* biofilms under controlled hydrodynamic conditions at 37 °C. Results suggested that biofilm viability measured with the plate reader agreed with those determined using plate counts and with the results of fluorescence microscope image analysis. Since then, the BioFlux system has been considered a high-throughput methodology for the study of biofilm development under defined hydrodynamic conditions [36, 49, 50, 52–54].

Although only 1 of 21 analysed studies had the specific objective of evaluating bacterial adhesion in urinary stents, all provided a comprehensive analysis of

adhesion and biofilm formation at flow conditions representative of relevant hydrodynamic regions of ureteral stents [55] and should be considered when testing a new surface or coating for these medical settings.

5 Operating Conditions

As previously shown, MRDs, flow chambers and microfluidic devices have been used to study bacterial adhesion and biofilm formation under hydrodynamic conditions that simulate the UTDs. Because the flow rate by itself provides little information about shear without taking into account the geometry of the *in vitro* flow system, it is crucial to mimic the flow conditions in a catheter or stent by using either the wall shear stress or the shear rate [1]. The wall shear rate (σ, with unit/s) is a measure of change of the fluid velocity near the wall of the tube in the radial direction toward the center of the tube. In laminar conditions, the shear rate is related to the force which the fluid flow exerts on the wall, expressed as shear stress (τ, with unit Pa), through $\tau = \mu \times \sigma$, where μ is the dynamic viscosity of the fluid (10^{-3} Pa s for water). In the flow systems under study, the flow rate should be adjusted to approach an average shear rate of around 15/s as an estimate of the intraluminal urine flow, based on predictable daily urine production and internal catheter diameter [15]. Nevertheless, urinary output values are highly variable and may reach more than 10 times the mean value [56], yielding a proportional increase in wall shear rate. Some authors performed FC tests at a shear rate of 33/s, which is higher than mean values but still within the range of shear rates found in urinary catheters [25].

Regarding the flow chamber system described in this work (Fig. 2), the numerical simulations indicated that the shear rate of 15/s reported for urinary flow in catheters can be attained at a flow rate of 2 mL/s [2, 9]. On the other hand, the average shear stress in problematic zones of ureteral stents that are prone to encrustation (0.024 Pa) [55] can be obtained by operating the PPFC system at a flow rate of 4 mL/s [21]. In the case of MRDs used by our research group, the recirculation flow rates can range from 5 [12] to 53 mL/s [13] to mimic the shear forces on urinary catheters, depending on the geometry of the flow cell.

PDMS-based microfluidic devices are usually designed for a particular application, having their own architecture and geometry with specific operating conditions. In the case of the commercially available BioFlux system, numerical simulations revealed that the average shear stress value of 0.02 Pa reported for ureteral stents [55] can be reached at a flow rate of 66 μL/h [52].

6 Strengths and Limitations of Flow Platforms

Among the advantages of flow systems are the ability to compare, for instance, the effect that different substrates, media and hydrodynamic conditions exert on a biofilm at different developmental stages. These dynamic models may also provide an evaluation of the effect that transiently occurring molecules, such as antibiotics or adherence inhibitors, have on biofilms. However, the technical disadvantages of flow reactors include increased experimental complexity as well as possible formation/trapping of air bubbles in the setup tubing (particularly severe in microfluidic systems), as this can affect flow and biofilm architecture [57].

Choosing the experimental platform for flow experiments determines what kind of data can be extracted, and care must be taken to ensure that the selected reactor fulfills the objectives of the experiments. The three platforms covered in this chapter (modified Robbins device, flow chamber and microfluidics-based device) have benefits and limitations, which are summarized in Table 4.

Table 4 Advantages and disadvantages of dynamic biofilm cultivation devices

Platform	Advantages	Disadvantages
Modified Robbins device	Large biomass produced	Low to medium throughput
	Large number of sampling ports available for analysis	Limited *in situ* biofilm visualization
	Can run for very long periods without intervention	Biofilm destruction during sampling for quantitative analysis
Flow chamber	Allows direct and nondestructive observation of biofilm development	Low throughput
	Optimized for online *in situ* microscopy	Inability to study adhesion to nontransparent surfaces
Microfluidics-based device	Noninvasive technique	Requires special equipment for manufacturing and running systems
	Allows real-time visualization of biofilm development	Clogging can occur due to small dimensions
	Requires small volumes	Laborious operation
	Can be custom-made for specific purposes	
	Rapid and precise analysis	
	Compatible with single cells analysis	

7 Conclusions

To evaluate the anti-adhesive and antimicrobial performance of novel biomedical materials, a number of flow devices have been designed to recreate *in vivo* flow conditions. Shear stress and flow rate can be accurately controlled and varied in these *in vitro* flow systems, which requires prior knowledge of the flow dynamics inside the platform. After limiting their operational range, modified Robbins devices, flow chambers and microfluidic devices are suggested as experimental set-ups to mimic the flow behavior in urinary catheters and stents.

Acknowledgements This work was financially supported by: LA/P/0045/2020 (ALiCE), UIDB/00511/2020, and UIDP/00511/2020 (LEPABE), funded by national funds through the FCT/MCTES (PIDDAC); Project PTDC/CTMCOM/4844/2020 funded by the Portuguese Foundation for Science and Technology (FCT); and by Project 2SMART (NORTE-01-0145-FEDER-000054), supported by Norte Portugal Regional Operational Programme (NORTE 2020), under the PORTUGAL 2020 Partnership Agreement, through the European Regional Development Fund (ERDF). L. C. Gomes and M. J. Romeu acknowledge FCT for the financial support of her work contract through the Scientific Employment Stimulus—Individual Call—[CEECIND/01700/2017] and for a PhD grant (SFRH/BD/140080/2018), respectively. R. Teixeira-Santos acknowledges the receipt of a junior researcher fellowship from the Project PTDC/BII-BIO/29589/2017—POCI-01-0145-FEDER-029589. Support from the EU COST Action ENIUS (CA16217) is also acknowledged.

References

1. Ramstedt M, Ribeiro IAC, Bujdakova H, Mergulhão FJ, Jordao L, Thomsen P, et al. Evaluating efficacy of antimicrobial and antifouling materials for urinary tract medical devices: challenges and recommendations. Macromol Biosci. 2019;19(5):e1800384.
2. Moreira JMR, Araújo JDP, Miranda JM, Simões M, Melo LF, Mergulhão FJ. The effects of surface properties on *Escherichia coli* adhesion are modulated by shear stress. Colloids Surf B Biointerfaces. 2014;123:1–7.
3. Teodósio JS, Simões M, Melo LF, Mergulhão FJ. Flow cell hydrodynamics and their effects on *E. coli* biofilm formation under different nutrient conditions and turbulent flow. Biofouling. 2011;27(1):1–11.
4. Pereira MO, Kuehn M, Wuertz S, Neu T, Melo LF. Effect of flow regime on the architecture of a *Pseudomonas fluorescens* biofilm. Biotechnol Bioeng. 2002;78(2):164–71.
5. De Grazia A, LuTheryn G, Meghdadi A, Mosayyebi A, Espinosa-Ortiz EJ, Gerlach R, et al. A microfluidic-based investigation of bacterial attachment in ureteral stents. Micromachines. 2020;11(4):408.
6. Pousti M, Zarabadi MP, Abbaszadeh Amirdehi M, Paquet-Mercier F, Greener J. Microfluidic bioanalytical flow cells for biofilm studies: a review. Analyst. 2019;144(1):68–86.
7. Lecuyer S, Rusconi R, Shen Y, Forsyth A, Vlamakis H, Kolter R, et al. Shear stress increases the residence time of adhesion of *Pseudomonas aeruginosa*. Biophys J. 2011;100(2):341–50.
8. Yang W, Zhou F. Polymer brushes for antibiofouling and lubrication. Biosurf Biotribol. 2017;3(3):97–114.
9. Moreira JMR, Ponmozhi J, Campos JBLM, Miranda JM, Mergulhão FJ. Micro- and macro-flow systems to study *Escherichia coli* adhesion to biomedical materials. Chem Eng Sci. 2015;126:440–5.

10. McCoy WF, Bryers JD, Robbins J, Costerton JW. Observations of fouling biofilm formation. Can J Microbiol. 1981;27(9):910–7.
11. Stoodley P, Warwood BK. Use of flow cells an annular reactors to study biofilms. In: Lens P, O'Flaherty V, Moran AP, Stoodley P, Mahony T, editors. Biofilms in medicine, industry and environmental biotechnology: characteristics, analysis and control. 1st ed. Cornwall: IWA Publishing; 2003. p. 197–213.
12. Azevedo AS, Almeida C, Gomes LC, Ferreira C, Mergulhão FJ, Melo LF, et al. An *in vitro* model of catheter-associated urinary tract infections to investigate the role of uncommon bacteria on the *Escherichia coli* microbial consortium. Biochem Eng J. 2017;118:64–9.
13. Vladkova T, Angelov O, Stoyanova D, Gospodinova D, Gomes LC, Soares A, et al. Magnetron co-sputtered TiO_2/SiO_2/Ag nanocomposite thin coatings inhibiting bacterial adhesion and biofilm formation. Surf Coat Technol. 2020;384:125322.
14. Tunney MM, Keane PF, Gorman SP. Assessment of urinary tract biomaterial encrustation using a modified Robbins device continuous flow model. J Biomed Mater Res. 1997;38(2):87–93.
15. Velraeds MMC, Van Der Mei HC, Reid G, Busscher HJ. Inhibition of initial adhesion of uropathogenic *Enterococcus faecalis* to solid substrata by an adsorbed biosurfactant layer from *Lactobacillus acidophilus*. Urology. 1997;49(5):790–4.
16. Teodósio JS, Simões M, Alves MA, Melo LF, Mergulhão FJ. Setup and validation of flow cell systems for biofouling simulation in industrial settings. Sci World J. 2012;2012:361496.
17. Teodósio JS, Silva FC, Moreira JMR, Simões M, Melo LF, Alves MA, et al. Flow cells as quasi-ideal systems for biofouling simulation of industrial piping systems. Biofouling. 2013;29(8):953–66.
18. Azeredo J, Azevedo NF, Briandet R, Cerca N, Coenye T, Costa AR, et al. Critical review on biofilm methods. Crit Rev Microbiol. 2017;43(3):313–51.
19. Alves P, Gomes LC, Vorobii M, Rodriguez-Emmenegger C, Mergulhão FJ. The potential advantages of using a poly(HPMA) brush in urinary catheters: effects on biofilm cells and architecture. Colloids Surf B Biointerfaces. 2020;191:110976.
20. Habash MB, Mei HCV, Busscher HJ, Reid G. The effect of water, ascorbic acid, and cranberry derived supplementation on human urine and uropathogen adhesion to silicone rubber. Can J Microbiol. 1999;45(8):691–4.
21. Dolid A, Gomes LC, Mergulhão FJ, Reches M. Combining chemistry and topography to fight biofilm formation: fabrication of micropatterned surfaces with a peptide-based coating. Colloids Surf B Biointerfaces. 2020;196:111365.
22. Vagos MR, Gomes M, Moreira JMR, Soares OSGP, Pereira MFR, Mergulhão FJ. Carbon nanotube/poly(dimethylsiloxane) composite materials to reduce bacterial adhesion. Antibiotics. 2020;9(8):434.
23. Vagos MR, Moreira JMR, Soares OSGP, Pereira MFR, Mergulhão FJ. Incorporation of carbon nanotubes in polydimethylsiloxane to control *Escherichia coli* adhesion. Polym Compos. 2019;40(S2):E1697–E704.
24. Alves P, Gomes LC, Rodríguez-Emmenegger C, Mergulhão FJ. Efficacy of a poly(MeOEGMA) brush on the prevention of *Escherichia coli* biofilm formation and susceptibility. Antibiotics. 2020;9(5):216.
25. Andersen TE, Kingshott P, Palarasah Y, Benter M, Alei M, Kolmos HJ. A flow chamber assay for quantitative evaluation of bacterial surface colonization used to investigate the influence of temperature and surface hydrophilicity on the biofilm forming capacity of uropathogenic *Escherichia coli*. J Microbiol Methods. 2010;81(2):135–40.
26. Alves P, Nir S, Reches M, Mergulhão FJ. The effects of fluid composition and shear conditions on bacterial adhesion to an antifouling peptide-coated surface. MRS Commun. 2018;8(3):938–46.
27. Gomes M, Gomes LC, Teixeira-Santos R, Mergulhão FJ. PDMS in urinary tract devices: applications, problems and potential solutions. In: Carlsen PN, editor. Polydimethylsiloxane: structure and applications. New York: Nova Science Publishers; 2020. p. 95–144.

28. Cattò C, Cappitelli F. Testing anti-biofilm polymeric surfaces: where to start? Int J Mol Sci. 2019;20(15):3794.
29. Tolker-Nielsen T, Sternberg C. Growing and analyzing biofilms in flow chambers. Curr Protoc Microbiol. 2011;21(1):1B.2.1–B.2.17.
30. Reichhardt C, Parsek MR. Confocal laser scanning microscopy for analysis of *Pseudomonas aeruginosa* biofilm architecture and matrix localization. Front Microbiol. 2019;10(677):677.
31. Thomas RN. *In situ* cell and glycoconjugate distribution in river snow studied by confocal laser scanning microscopy. Aquat Microb Ecol. 2000;21(1):85–95.
32. Heydorn A, Nielsen AT, Hentzer M, Sternberg C, Givskov M, Ersbøll BK, et al. Quantification of biofilm structures by the novel computer program COMSTAT. Microbiology. 2000;146(Pt10):2395–407.
33. Mueller LN, de Brouwer JFC, Almeida JS, Stal LJ, Xavier JB. Analysis of a marine phototrophic biofilm by confocal laser scanning microscopy using the new image quantification software PHLIP. BMC Ecol. 2006;6(1):1.
34. Gomes LC, Deschamps J, Briandet R, Mergulhão FJ. Impact of modified diamond-like carbon coatings on the spatial organization and disinfection of mixed-biofilms composed of *Escherichia coli* and *Pantoea agglomerans* industrial isolates. Int J Food Microbiol. 2018;277:74–82.
35. Lee JH, Kaplan JB, Lee WY. Microfluidic devices for studying growth and detachment of *Staphylococcus epidermidis* biofilms. Biomed Microdevices. 2008;10(4):489–98.
36. Tremblay YD, Vogeleer P, Jacques M, Harel J. High-throughput microfluidic method to study biofilm formation and host–pathogen interactions in pathogenic *Escherichia coli*. Appl Environ Microbiol. 2015;81(8):2827–40.
37. Shields RC, Burne RA. Growth of *Streptococcus mutans* in biofilms alters peptide signaling at the sub-population level. Front Microbiol. 2016;7:1075.
38. Ponmozhi J, Moreira JMR, Mergulhão FJ, Campos JBLM, Miranda JM. Fabrication and hydrodynamic characterization of a microfluidic device for cell adhesion tests in polymeric surfaces. Micromachines. 2019;10(5):303.
39. Neves SF, Ponmozhi J, Mergulhão FJ, Campos JBLM, Miranda JM. Cell adhesion in microchannel multiple constrictions—evidence of mass transport limitations. Colloids Surf B Biointerfaces. 2020;198:111490.
40. Rusconi R, Guasto JS, Stocker R. Bacterial transport suppressed by fluid shear. Nat Phys. 2014;10(3):212–7.
41. Secchi E, Vitale A, Miño GL, Kantsler V, Eberl L, Rusconi R, et al. The effect of flow on swimming bacteria controls the initial colonization of curved surfaces. Nat Commun. 2020;11(1):2851.
42. Siryaporn A, Kim MK, Shen Y, Stone HA, Gitai Z. Colonization, competition, and dispersal of pathogens in fluid flow networks. Curr Biol. 2015;25(9):1201–7.
43. Zhang XY, Sun K, Abulimiti A, Xu PP, Li ZY. Microfluidic system for observation of bacterial culture and effects on biofilm formation at microscale. Micromachines. 2019;10(9):606.
44. Janakiraman V, Englert D, Jayaraman A, Baskaran H. Modeling growth and quorum sensing in biofilms grown in microfluidic chambers. Ann Biomed Eng. 2009;37(6):1206–16.
45. Kim MK, Drescher K, Pak OS, Bassler BL, Stone HA. Filaments in curved streamlines: rapid formation of *Staphylococcus aureus* biofilm streamers. New J Phys. 2014;16(6):065024.
46. Weaver WM, Milisavljevic V, Miller JF, Di Carlo D. Fluid flow induces biofilm formation in *Staphylococcus epidermidis* polysaccharide intracellular adhesin-positive clinical isolates. Appl Environ Microbiol. 2012;78(16):5890–6.
47. Zarabadi MP, Paquet-Mercier F, Charette SJ, Greener J. Hydrodynamic effects on biofilms at the biointerface using a microfluidic electrochemical cell: case study of *Pseudomonas* sp. Langmuir. 2017;33(8):2041–9.
48. Kim MK, Ingremeau F, Zhao A, Bassler BL, Stone HA. Local and global consequences of flow on bacterial quorum sensing. Nat Microbiol. 2016;1:15005.
49. Moormeier DE, Endres JL, Mann EE, Sadykov MR, Horswill AR, Rice KC, et al. Use of microfluidic technology to analyze gene expression during *Staphylococcus aureus* biofilm formation reveals distinct physiological niches. Appl Environ Microbiol. 2013;79(11):3413–24.

50. Lehman MK, Bose JL, Sharma-Kuinkel BK, Moormeier DE, Endres JL, Sadykov MR, et al. Identification of the amino acids essential for LytSR-mediated signal transduction in *Staphylococcus aureus* and their roles in biofilm-specific gene expression. Mol Microbiol. 2015;95(4):723–37.
51. Benoit MR, Conant CG, Ionescu-Zanetti C, Schwartz M, Matin A. New device for high-throughput viability screening of flow biofilms. Appl Environ Microbiol. 2010;76(13):4136–42.
52. Feng SH, Stojadinovic A, Izadjoo M. Distinctive stages and strain variations of *A. baumannii* biofilm development under shear flow. J Wound Care. 2013;22(4):173–4.
53. Vanhommerig E, Moons P, Pirici D, Lammens C, Hernalsteens J-P, De Greve H, et al. Comparison of biofilm formation between major clonal lineages of methicillin resistant *Staphylococcus aureus*. PLoS One. 2014;9(8):e104561.
54. Goetz C, Tremblay YDN, Lamarche D, Blondeau A, Gaudreau AM, Labrie J, et al. Coagulase-negative staphylococci species affect biofilm formation of other coagulase-negative and coagulase-positive staphylococci. J Dairy Sci. 2017;100(8):6454–64.
55. Mosayyebi A, Yue QY, Somani BK, Zhang X, Manes C, Carugo D. Particle accumulation in ureteral stents is governed by fluid dynamics: in vitro study using a "stent-on-chip" model. J Endourol. 2018;32(7):639–46.
56. Fallis WM. Indwelling Foley catheters: is the current design a source of erroneous measurement of urine output? Crit Care Nurse. 2005;25(2):44–6.
57. Magana M, Sereti C, Ioannidis A, Mitchell CA, Ball AR, Magiorkinis E, et al. Options and limitations in clinical investigation of bacterial biofilms. Clin Microbiol Rev. 2018;31(3):e00084–16.
58. Lopez-Mila B, Alves P, Riedel T, Dittrich B, Mergulhão FJ, Rodriguez-Emmenegger C. Effect of shear stress on the reduction of bacterial adhesion to antifouling polymers. Bioinspir Biomim. 2018;13(6):065001.
59. Fundeanu I, van der Mei HC, Schouten AJ, Busscher HJ. Polyacrylamide brush coatings preventing microbial adhesion to silicone rubber. Colloids Surf B Biointerfaces. 2008;64(2):297–301.
60. Cringus-Fundeanu I, Luijten J, van der Mei HC, Busscher HJ, Schouten AJ. Synthesis and characterization of surface-grafted polyacrylamide brushes and their inhibition of microbial adhesion. Langmuir. 2007;23(9):5120–6.
61. Roosjen A, Kaper HJ, van der Mei HC, Norde W, Busscher HJ. Inhibition of adhesion of yeasts and bacteria by poly(ethylene oxide)-brushes on glass in a parallel plate flow chamber. Microbiology. 2003;149(11):3239–46.
62. Millsap K, Reid G, van der Mei HC, Busscher HJ. Displacement of *Enterococcus faecalis* from hydrophobic and hydrophilic substrata by *Lactobacillus* and *Streptococcus* spp. as studied in a parallel plate flow chamber. Appl Environ Microbiol. 1994;60(6):1867–74.
63. Gabi M, Hefermehl L, Lukic D, Zahn R, Vörös J, Eberli D. Electrical microcurrent to prevent conditioning film and bacterial adhesion to urological stents. Urol Res. 2011;39(2):81–8.